Article

Future changes in South Asian summer monsoon circulation under global warming: role of the Tibetan Plateau latent heating

Check for updates

Haolin Luo[1], Ziqian Wang [1,2] ✉, Chao He [3], Deliang Chen [4] & Song Yang [1,2] ✉

The South Asian summer monsoon (SASM) is a significant monsoon system that exerts a profound impact on climate and human livelihoods. According to 38 models from the Coupled Model Intercomparison Project Phase 6, the SASM circulation is projected to weaken significantly under global warming as seen in the weakened low-level westerly wind over the northern tropical Indian Ocean; however, the associated climate dynamics is still under debate. Here, we identify that the weakened low-level westerly wind is closely related to the enhanced latent heating over the Tibetan Plateau (TP), which corresponds with increased summer precipitation in the future. The intensified TP latent heating triggers an anomalous meridional circulation with ascending motions over the plateau and descending motions to the south, leading to an anomalous low-level anticyclone over the northern tropical Indian Ocean. This anticyclone greatly weakens the prevailing low-level westerlies of the SASM through easterly anomalies at the anticyclone's southern flank. Moisture budget analysis further reveals that increased atmospheric water vapor, rather than the vertical dynamic component, makes the largest contribution to the increased precipitation over the TP. This result confirms that the enhanced TP latent heating is a driver of atmospheric circulation change and contributes to weakening the SASM circulation.

The South Asian summer monsoon (SASM) is a prominent monsoon system characterized by prevailing westerly wind in the lower troposphere, and is considered one of the most spectacular monsoon systems in the world[1–3]. The SASM brings abundant precipitation to South Asia (SA), providing a major water resource and sustaining billions of people in the region[4,5]. The SASM is also critical for production of wind power, which satisfies the urgent demand for renewable energy in SA[6]. The variation of the SASM exerts a great impact on natural ecosystems, food security, and social economy in relevant countries[7–10]. Understanding the physical mechanism for the SASM response to global warming is of great importance for climate adaptation and government policy.

Previous studies show that the SASM has experienced a significant weakening trend in both precipitation and circulation over the twentieth century[11,12], but with a recovery in recent decades[12,13]. However, there exists a notable paradox about the future changes in SASM precipitation and circulation. While SASM precipitation is projected to possess a robust increase in the face of ongoing global warming[14,15], several studies have documented a notable weakening in SASM circulation, characterized by anomalous low-level easterly wind in northern tropical Indian Ocean[3,16–22]. The enhanced precipitation is mainly owing to the increased moisture in the warmer atmosphere, following the "wet-gets-wetter" pattern[23–26]. The decline in SASM circulation has been attributed to a variety of potential factors, including the reduction of meridional land–sea thermal contrast in the upper troposphere[27–30], the mean advection of stratification change[31,32], the enhanced precipitation over North Africa (NA)[33], and the suppressed convection over the Maritime Continent (MC)[33–35]. Since the SASM is a

[1]School of Atmospheric Sciences, Sun Yat-sen University and Southern Marine Science and Engineering Guangdong Laboratory (Zhuhai), Zhuhai, China. [2]Guangdong Province Key Laboratory for Climate Change and Natural Disaster Studies, Sun Yat-sen University, Zhuhai, China. [3]Institute for Environmental and Climate Research, Jinan University, Guangzhou, China. [4]Regional Climate Group, Department of Earth Sciences, University of Gothenburg, Gothenburg, Sweden. ✉e-mail: wangziq5@mail.sysu.edu.cn; yangsong3@mail.sysu.edu.cn

complex and interconnected system involving oceanic, atmospheric, and terrestrial processes on multiple scales, comprehensively understanding the mechanisms behind the anticipated weakening of SASM circulation remains an ongoing challenge.

Located in the subtropical central-eastern Eurasian continent, the Tibetan Plateau (TP) is the highest plateau in the world, with an average altitude exceeding 4 km. Due to its unique location and high elevation, the TP exerts a profound influence on the regional and even global climate through its mechanical and thermal forcings[36–45]. In summer, the TP serves as a huge elevated heat source[46,47], which is able to directly heat the air in the middle troposphere[48,49], modulating the onset, duration, and structure of the SASM[50–52]. According to the Intergovernmental Panel on Climate Change (IPCC) Sixth Assessment Report (AR6), mountain areas are highly sensitive and vulnerable to climate change[53]. Since the global warming has accelerated the water cycle over the TP in the past decades[54] and is projected to continue in the 21st century[53], the TP is considered one of the hotspots worth substantial attention[51,55]. As an important part of the water cycle process, precipitation is projected to increase obviously, especially during the summer monsoon season[56,57]. The latent heat released by the increased precipitation then enhances the local elevated heat source over the TP, which is likely to play an indispensable role in the future atmospheric circulation around the TP[56].

Previous studies have confirmed the important role of TP heating in the formation of SASM[36,37,39,40], specifically the northern branch of the SASM. As a basic trigger, the topographically elevated surface sensible heating drives surrounding low-level water vapor to converge toward the TP, much like a sensible-heat-driven air-pump[40,51]. Subsequently, the converged water vapor is uplifted to produce heavy precipitation and release considerable latent heating over the TP. Then huge TP heating in summer generates and strengthens the northern branch (north of 20°N) of the SASM[42]. In this current study, we re-examine the projected changes in SASM circulation and summer heat condition of the TP based on 38 models in the latest Coupled Model Intercomparison Project Phase 6 (CMIP6). We identify that one of the main features of the projected SASM circulation is the weakened low-level westerly wind over the northern tropical Indian Ocean (55°E–100°E, 3°N–15°N), as we will discuss later in Fig. 1c. Further investigation reveals that there exists a significant correlation between the weakened SASM circulation and enhanced thermal forcing over the TP

from the perspective of both seasonal consistency and inter-model spread. We emphasize that the enhanced TP thermal forcing will strengthen the northern branch of SASM circulation in future, but weaken the southern branch by triggering anomalous meridional circulation, which finally declines the low-level westerly wind over the northern tropical Indian Ocean and the SASM circulation as a whole.

Results

Projected changes under global warming

How will the South Asian Summer Monsoon (SASM) circulation and Tibetan Plateau (TP) summer precipitation change in the context of global warming? We use data from 38 CMIP6 models and the resulting future projections to construct SASM circulation indices (including the low-level zonal wind index (SASMI), vertical wind shear index (VWSI), and meridional wind shear index (MWSI)) and TP precipitation index (TPPI) (see Methods) as presented in Fig. 1a, relative to the historical mean of 1965–2014. All three monsoon indices consistently exhibit a significant decreasing trend in the future, with multi-model ensemble (MME) mean values of -0.15, -0.52, and -0.18 m s^{-1} per decade since 2015, which are statistically significant at the 99% confidence level. By the second half of this century (2050–2099), the SASM circulation is projected to weaken by -11.0%, -13.5%, and -23.2% in the three indices, respectively, compared to their climatological means of 1965–2014 (Fig. 1b). These quantitative findings warrant close attention and vigilance. In contrast, the anomalous summer precipitation over the TP is projected to increase with a growth rate of 0.20 mm day^{-1} per decade and shows a notable percentage change of 19.4%. During summer, the heat source over the TP is primarily fueled by the substantial latent heat released from abundant precipitation[58–60]. The projected enhancement of latent heating is much larger than the weak changes in sensible heating and radiation cooling over the TP, completely dominating the increase in total diabatic heating (Supplementary Fig. 1a). Meanwhile, the correlation coefficient between the change in TPPI and the total heating over the TP is up to 0.97 among 38 models (Supplementary Fig. 1b), suggesting that the precipitation and associated latent heating are reliable indicators for the projected TP thermal forcing.

Further insight into why the monsoon indices weaken in the future can be gained by examining the spatial pattern of low-level circulation. The most striking feature is a large-scale anomalous anticyclone over SA in the 850-hPa

Fig. 1 | Projected changes under global warming. a Time series of SASMI, VWSI, MWSI (m s^{-1}) and TPPI (mm day^{-1}) anomalies, relative to the mean of 1965–2014. **b** Percentage changes (%) in SASMI, VWSI, MWSI and TPPI averaged during 2050–2099 and comparison with 1965–2014. **c** Projected changes in the precipitation (shading, mm day^{-1}) and 850-hPa winds (vectors, m s^{-1}) during 2050–2099 under the SSP5-8.5 scenarios, relative to 1965–2014. In (**a**), the shadings represent the 30th and 70th percentiles among 38 models and the gray shading bar indicates the dividing time for the historical and SSP5-8.5 simulations. In (**b**), the box-whisker denotes the 10th, 30th, MME, 70th, and 90th percentiles of the 38 models. In (**c**), the stippling and black vectors denote where at least 70% of the individual models agree in sign with the MME-projected values in precipitation and winds, respectively; the red curves denote the topography with a height of 1500 m; and the blue and purple rectangles denote the TP (75°E–102°E, 25°N–37°N) and the key region for the SASM (55°E–100°E, 3°N–15°N).
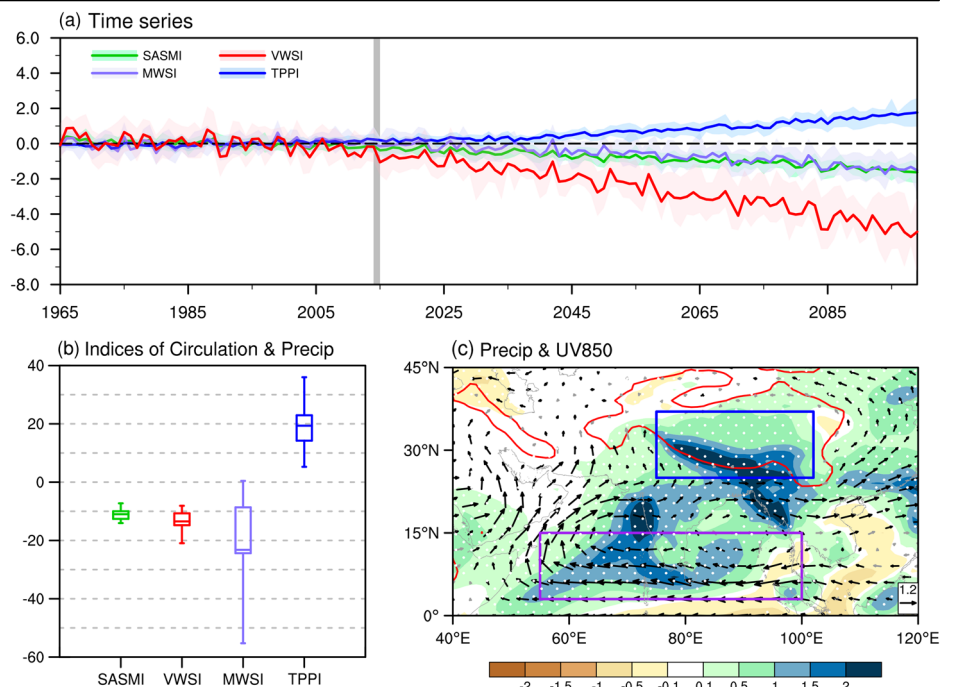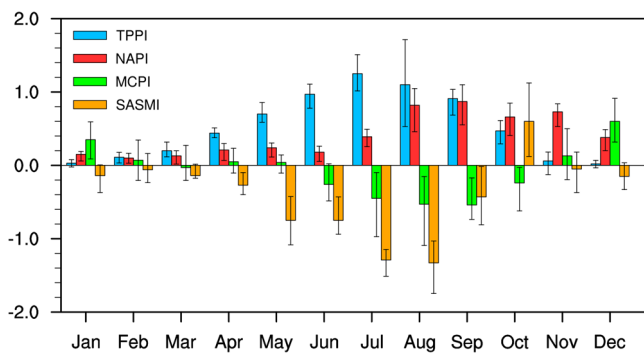
Fig. 2 | Seasonality of the projected changes in the SASM circulation and summer precipitation over the TP, NA, and MC. Annual cycles of the monthly projected changes in SASMI (m s^{-1}) and TPPI, MCPI, and NAPI (mm day^{-1}), based on the comparison between 2050–2099 and 1965–2014. The whisker denotes the inter-model spread shown by the 30th and 70th percentiles among 38 models.

circulation, supported by more than 70% of individual models (Fig. 1c). Easterly anomalies are apparent on the southern flank of this anomalous anticyclone (purple box, 55°E–100°E, 3°N–15°N), an area where climatological low-level westerly wind prevails during the SASM season. This situation results in a notable weakening of the whole SASM circulation. However, the precipitation over SA displays a significant increase, with two prominent centers over the western Indian subcontinent and the northwest of the Indochina Peninsula (Fig. 1c), aligning with a wetter future for South Asia suggested by earlier studies[14,15,30]. Meanwhile, TP precipitation (blue box, 75°E–102°E, 25°N–37°N) shows a robust increase, with the most significant positive values in the southern part, corresponding to the climatological monsoon precipitation center[61].

Connection between weakened SASM circulation and enhanced latent heating over the TP

The anomalous anticyclone in the lower troposphere (Fig. 1c) has been previously shown in numerical experiments studying the atmospheric responses to thermal forcing of the TP (see Fig. 2 in He et al.[62] and Fig. 2 in Wang et al.[63]). This finding prompts considerations of a potential correlation between the changes in TP latent heating and the SASM circulation under global warming. Furthermore, Li et al.[33] have suggested that the weakened SASM circulation may be attributed to a negative heating anomaly over the Maritime Continent (MC) through the Gill response. They also proposed that the enhanced latent heat over North Africa (NA) could stimulate Kelvin waves to the east. Both the MC negative heating and the NA enhanced heating stimulate a response of anomalous low-level easterlies in the northern tropical Indian Ocean, contributing to the weakened SASM circulation.

Here, we examine the monthly evolutions of projected changes in SASMI, TPPI, Maritime Continent precipitation index (MCPI), and North Africa precipitation index (NAPI) (Fig. 2; see "Methods"). Notably, distinctive easterly anomalies associated with the weakened SASM circulation are prevalent in May, June, July, and August, with relatively small values or even opposite trends in other months. While the SASMI change is notably high in May, our primary focus is on the main SASM period from June to August (JJA). Interestingly, the TPPI anomalies also exhibit greater magnitudes during the summer months compared to other seasons. Consequently, the season demonstrating the most pronounced easterly anomalies over southern SA also displays the most significant increase in precipitation and latent heat over the TP, suggesting a consistent seasonality between the weakened SASM circulation and the enhanced TP thermal forcing. However, the NAPI anomaly peaks in late summer and autumn, with much smaller values in June and July, contradicting the period when the SASM circulation weakens the most. Similarly, the most intense negative precipitation (latent heating) anomaly over the MC occurs in September, while the SASMI only exhibits a relatively small weakening trend at the same time

compared to summer. This seasonality is also evident when the monsoon index is switched to VWSI or MWSI (Supplementary Fig. 2), indicating the robustness of the result. Motivated by the seasonal consistency, we further investigate the potential relationship from the perspective of inter-model variations. The scatter diagram among the 38 models is presented in Fig. 3, which shows that the TPPI is strongly correlated with all three circulation indices of the SASM (SASMI, VWSI, and MWSI), with correlation coefficients of -0.55, -0.52, and -0.53, respectively, all of which significantly exceed the 99% confidence level. These significant negative relationships suggest that a model projecting a larger increase in TP precipitation tends to forecast a more pronounced weakening of the SASM circulation. This feature also indicates that the inter-model uncertainty regarding the changes in SASM circulation can be partially explained by the variation of TP latent heating anomalies among the models.

Physical mechanism for the effect of enhanced TP latent heating on the weakened SASM circulation

Building upon the observed seasonal consistency and inter-model variability, we confirm a significant relationship between enhanced TP latent heating and weakened SASM circulation. However, the physical mechanism for the influence of TP thermal forcing on SASM circulation in a warming world still remains unclear. Climatologically, the vertical structure of SASM circulation is characterized by robust upward motions from the tropical Indian Ocean to the TP (Supplementary Fig. 3). However, the projected change reveals a marked anomalous meridional circulation, featuring deep rising motions over the southern TP and noticeable sinking motions roughly between 10°N and 20°N (Fig. 4a). The descending branch of this anomalous meridional circulation aligns with the center of the low-level anomalous anticyclone, indicating a potential link between these two systems. Previous studies have suggested that the diabatic heating over the TP can induce vigorous upward motions, which may directly instigate regional meridional circulation to the south[51,64]. Consequently, we analyze the regressions of the projected changes in meridional circulation against the normalized TP precipitation index (TPPI) among the 38 models to elucidate the circulation patterns associated with TP latent heating (Fig. 4b; see "Methods"). In a manner consistent with the projected result from the CMIP6 MME (Fig. 4a), an anomalous meridional circulation extending from the TP to SA is observed. The intensified latent heating over the TP is linked to robust upward motions along the southern slope of the plateau and prominent descending motions in the southern region. This pattern may lead to subsequent divergence and the emergence of an anomalous anticyclone in the lower troposphere over SA. Figure 4c demonstrates the regressions of projected changes in precipitation and 850-hPa winds onto the normalized TPPI among the 38 models. As TP precipitation increases, particularly along the southern slope (within the blue box in Fig. 4c), a large-scale anomalous anticyclone emerges over SA, resembling the projected MME circulation pattern depicted in Fig. 1c. Along the southern branch of this anomalous anticyclone, easterly anomalies prevail from the southern Bay of Bengal to the southern Arabian Sea (within the purple box in Fig. 4c), which in turn weaken the prevailing low-level westerly wind of the SASM in these regions.

To validate the above diagnostic result, we conduct a pair of numerical experiments using the Community Earth System Model (CESM): a control run "**Con**" and a sensitivity run with prescribed TP heating "**TPheat**" (see details in "Methods"). Figure 5a illustrates the projected changes in summer diabatic heating (see "Methods") over the TP and its surrounding areas in the CMIP6 MME. The results show significantly enhanced heating over the TP, which aligns with the distribution of precipitation change. This consistency confirms the dominant role of latent heat in the total diabatic heating in summer. The maximum heating above the TP is found at approximately 500 hPa (Fig. 5b), conforming the characteristics of the latent heat released by convective precipitation. This vertical profile of the projected change in Q1 (see "Methods") over the TP is added to the **TPheat** experiment.

Figure 5c presents the differences in summer 850-hPa winds and precipitation between experiment **TPheat** and control run **Con**. The circulation

Fig. 3 | Relationship between the changes in summer precipitation over the TP and SASM circulation. Inter-model relationships between the projected changes in TPPI (mm day^{-1}) and (**a**) SASMI (m s^{-1})/(**b**) VWSI (m s^{-1})/(**c**) MWSI (m s^{-1}) during 2050–2099 under the SSP5-8.5 scenarios, relative to 1965–2014.
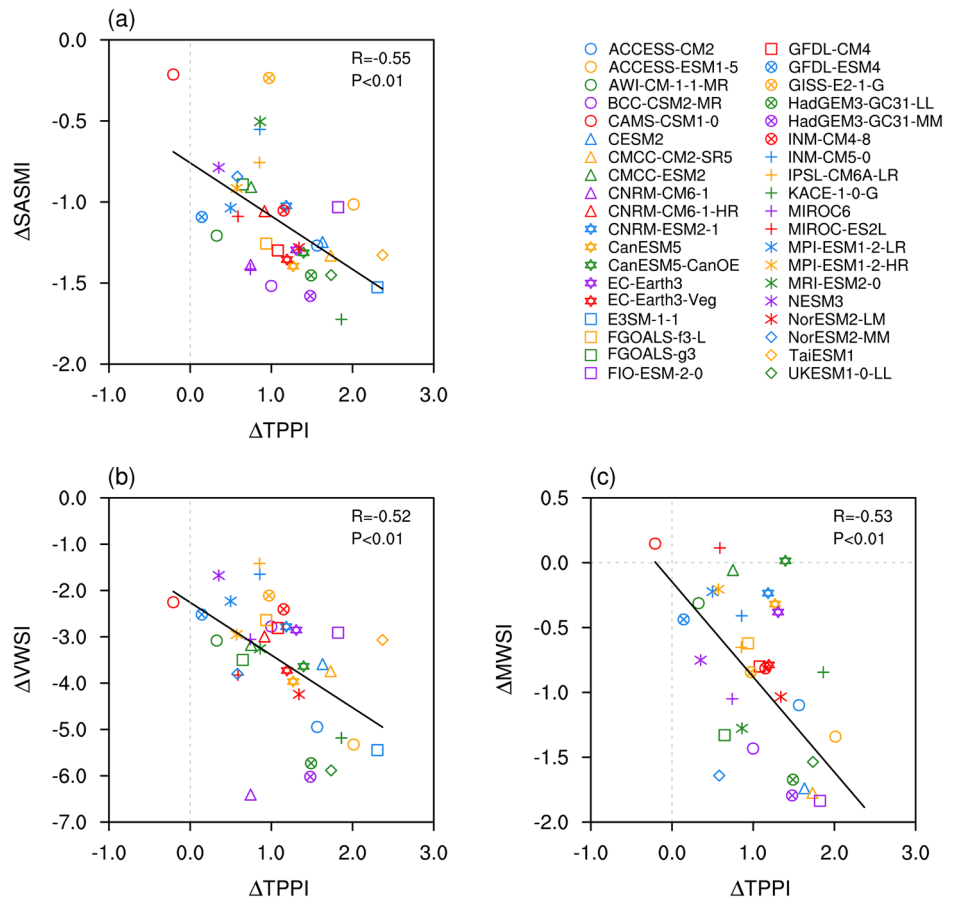
response to the TP heating in CESM closely resembles the patterns of MME changes (Fig. 1c) and the inter-model regressed features (Fig. 4c). An anomalous anticyclone over southern SA is well-replicated, with easterly anomalies along its southern branch (within the purple box in Fig. 5c), opposite with the climatological low-level westerly wind of the SASM. By examining the differences in meridional circulation (Fig. 5d), we can elucidate the detailed mechanism underlying the formation of the low-level anomalous anticyclone. Abundant air is lifted due to the elevated thermal forcing from the TP, leading to upper-level outflow and subsequent convergence at the lower latitudes. This situation results in significant anomalous descending motions in the region. Subsequently, the divergent air in the lower troposphere triggers the formation of an anomalous anticyclone over southern SA, which is considered a key factor in weakening the SASM circulation.

It is worth noting that the sensitivity experiment shows decreased precipitation over SA when additional TP heating is prescribed (Fig. 5c), which seems contradictory to the projected change in CMIP6 (Fig. 1c). In the next section, we will investigate the potential causes for the future precipitation changes over the TP and SA under global warming, respectively.

Moisture budget analysis on the projected change in precipitation

Precipitation and ascending motions are intertwined, acting as both causes and effects of one another. To elaborate, precipitation formation releases latent heat, which directly warms the atmosphere and triggers local upward motions. Conversely, ascending motions provide conducive dynamic conditions for water vapor to condense into precipitation. This interplay might raise the question of whether the robust upward motions are the cause, rather than the consequence, of the increased precipitation over the TP. To address this question, we quantitatively dissect the increased precipitation

over the TP into various contributors using the atmospheric moisture budget equation (Fig. 6a; see "Methods").

We can clearly see that the thermodynamic term of the vertical moisture advection $\left(-\left\langle\bar{\omega}\frac{\partial q'}{\partial p}\right\rangle\right)$ makes the largest positive contribution over the TP, which is mainly attributed to the increased water vapor. Previous studies have considered the enhanced moisture as a response to the global warming following the Clausius-Clapeyron relation[21,23,65]. The enhanced evaporation also makes a considerably positive contribution, implying an intensified hydrological recycling over the TP[54,56]. Meanwhile, it is clear that the dynamic component of vertical moisture advection associated with the change in vertical motions $\left(-\left\langle\omega'\frac{\partial\bar{q}}{\partial p}\right\rangle\right)$ shows little contribution, along with the obvious ascending motions forced by the TP heating in CESM experiments, suggesting that the strong ascent over the TP is a result of the increased precipitation, instead of the cause. Therefore, the enhanced TP latent heating triggers intense ascending motions above and further leads to descending motions over SA through anomalous meridional circulation. We also calculate the components in moisture budget equation over SA (60°E–100°E, 10°N–20°N). Similarly, the vertical thermodynamic term $\left(-\left\langle\bar{\omega}\frac{\partial q'}{\partial p}\right\rangle\right)$ is the largest contributor to the enhanced precipitation over SA as the atmospheric moisture increases under global warming. However, the vertical dynamic component $\left(-\left\langle\omega'\frac{\partial\bar{q}}{\partial p}\right\rangle\right)$ presents a negative contribution due to the descending motions over SA, which is dynamically unfavorable for precipitation. The moisture budget in the CESM simulation is further analyzed (Supplementary Fig. 4), in which the atmospheric response to the TP latent heating alone is reflected. Without the increased moisture due to global warming as in the CMIP6 projection, the precipitation over SA significantly decreases owing to the large negative contribution of the anomalous descending motions, which explains the inconsistency between the CMIP6 (Fig. 1c) and the CESM (Fig. 5c) in the precipitation patterns over SA.

Fig. 4 | SASM circulation and precipitation changes in the MME projection and the inter-model regression. a Projected changes in vertical velocity (shading, 50 Pa s^{-1}) and meridional circulation (vectors, units of meridional wind and vertical velocity are in m s^{-1} and −50 Pa s^{-1}, respectively) averaged over 75°E–100°E. **b, c** are the same as (**a**) and Fig. 1c, respectively, but for the inter-model regression patterns against the normalized changes in TPPI among 38 models. In (**a**), the stippling (for the shading) and black vectors denote where at least 70% of the individual models agree in sign with the MME-projected values and the gray shading indicates the topography. In (**b**) and (**c**), the stippling (for the shading) and black vectors denote the significant values exceeding the 90% confidence level.
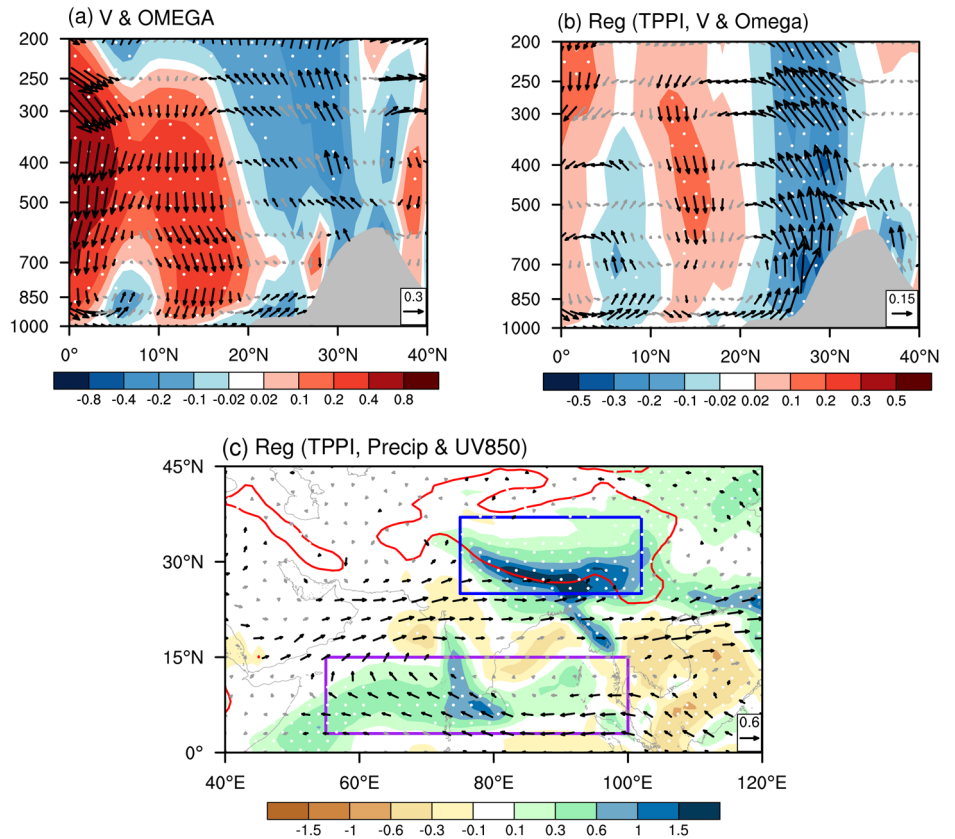

Fig. 5 | Projected TP diabatic heating and its forced response of the SASM in sensitivity experiments. a Projected change in the vertically integrated *Q1* (shading, K day^{-1}) from surface to 100 hPa during 2050–2099 under the SSP5-8.5 scenarios, relative to 1965–2014. **b** Vertical profile of the projected change in *Q1* (K day^{-1}) averaged over the TP area (bule rectangle in (**a**); 75°E–102°E, 25°N–37°N). **c** Differences in the precipitation (shading, mm day^{-1}) and 850-hPa winds (vectors, m s^{-1}) between experiment **TPheat** and experiment **Con**. **d** The same as (**c**), but for the vertical velocity (shading, 50 Pa s^{-1}) and meridional circulation (vectors, units of meridional wind and vertical velocity are in m s^{-1} and −50 Pa s^{-1}, respectively) averaged over 75°E–100°E. In (**c**), the purple rectangles denote the key region for the SASM (55°E–100°E, 3°N–15°N); and the red curves denote the topography with a height of 1500 m. In (**c, d**), the stippling (for the shading) and black vectors denote the significant values exceeding the 90% confidence level and the gray shading indicates the topography.
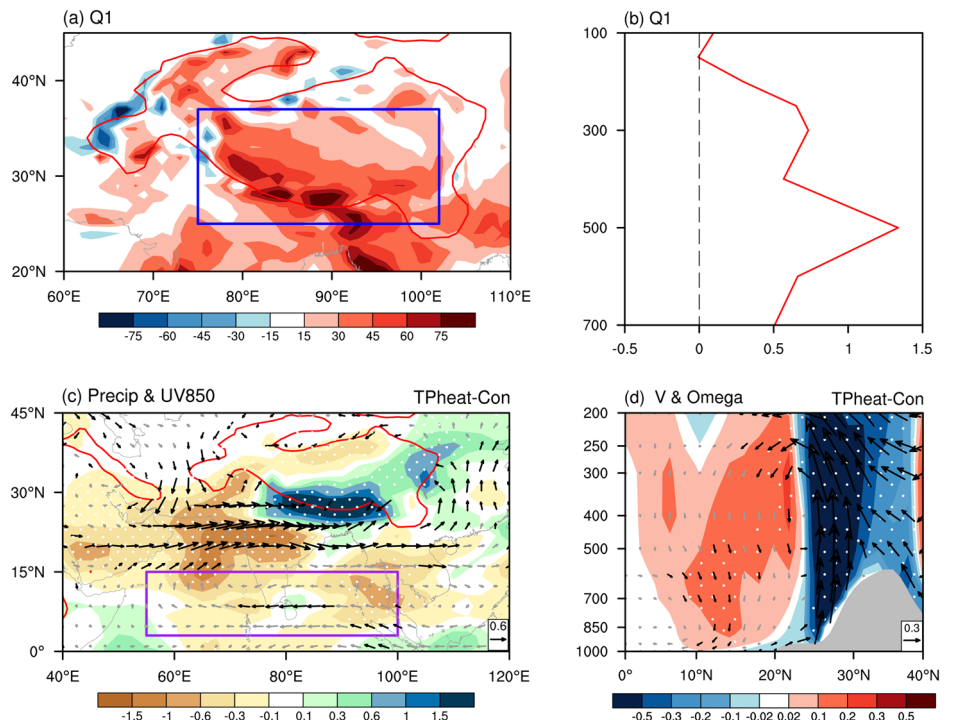
Discussion

Based on the latest CMIP6 output and numerical experiments, our study demonstrates the indispensable role of the summer-enhanced precipitation or diabatic heating over the TP in weakening the SASM circulation under global warming. The detailed physical mechanism is summarized schematically in Fig. 7. Global warming results in increased water vapor over the TP, driving both enhanced precipitation and more potent thermal forcing. Consequently, warm air rises, and the southward airflow, stemming from
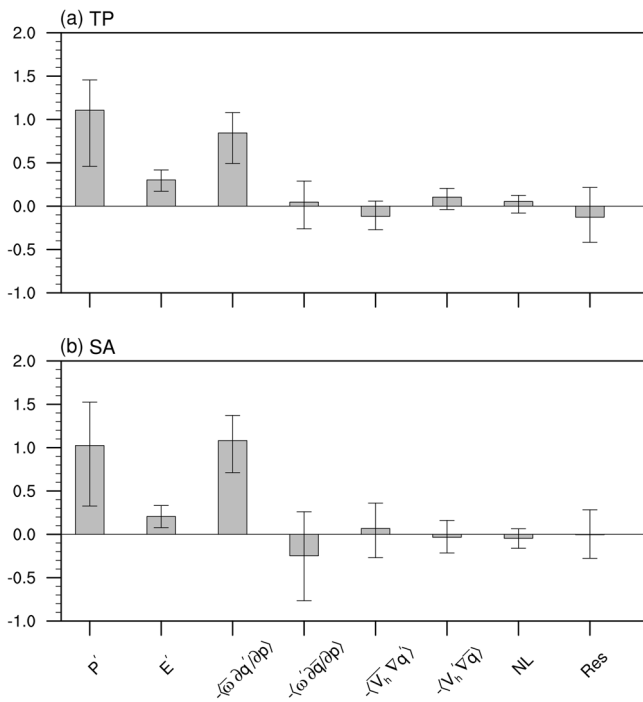
Fig. 6 | Moisture budget on the changes in summer precipitation over the TP and SA. Projected changes in the terms in moisture budget equation averaged over (**a**) TP (75°E–102°E, 25°N–37°N) and (**b**) SA (60°E–100°E, 10°N–20°N). The whisker denotes the inter-model spread shown by the 30th and 70th percentiles among 38 models.
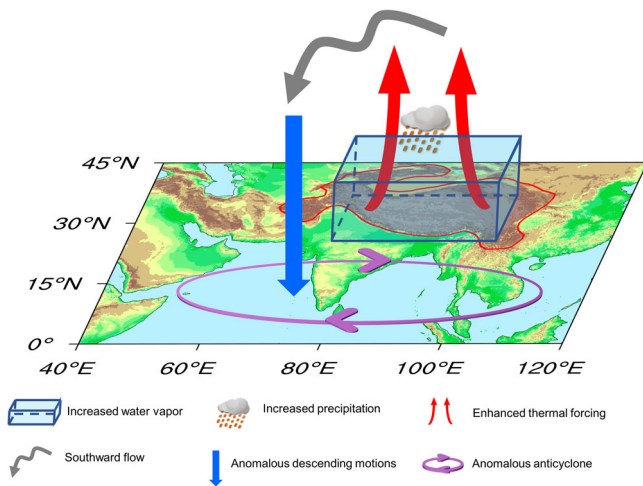

Fig. 7 | Summary schematic. Schematic diagram showing the physical mechanism for the effect of the enhanced TP thermal forcing in summer on SASM circulation under global warming.

the upper tropospheric divergence, descends over South Asia, forming an anomalous large-scale anticyclone at the lower levels. This anticyclone weakens the prevailing westerly wind of the SASM through the presence of anomalous easterlies in the southern flank of this anticyclone.

It is commonly accepted that the TP thermal forcing plays an important role in the formation of SASM[40,42,51], especially in generating and strengthening its northern branch over the southern TP. In this study, we emphasize that the projected enhanced TP latent heating will also strengthen the local upward motions in a warming world, corresponding with the northern branch of the SASM, which is in line with the traditional view. Indeed, previous studies have revealed a poleward shift of the SASM

circulation, characterized by strengthened monsoon westerly wind over the northern SA, and attributed this shift to the enhanced surface land-sea thermal contrast[32,65]. Here, we suggest the nonnegligible role of the TP latent heating in shifting the SASM circulation to the north under global warming. It can be clearly seen that anomalous westerly wind prevails at the northern flank of the anomalous low-level anticyclone emphasized in this study, which can intensify the climatological low-level westerly wind of the northern SASM. Meanwhile, a significant large-scale cyclone around the TP topography is observed in the CESM simulation (Fig. 5c), which is forced by the enhanced TP heating[56,63]. The low-level westerly wind at the southern branch of the anomalous cyclone around the topography can also intensify the monsoon westerly wind over northern SA. Climatologically, the vertical structure of the SASM can be usually divided into two distinctive branches[51], with one at the south of 20°N and the other at the southern TP (Supplementary Fig. 3). In the context of global warming, the anomalous meridional circulation induced by the enhanced TP latent heating strengthens the northern branch but weakens the southern one, further leading to a poleward shift of the SASM circulation.

Regional climate change results from a complex interplay between anthropogenic influence and natural variability[61,66,67]. For example, a recent study has revealed that the precipitation over the TP exhibits a dipolar pattern with drying in the south and wetting in the northwest during the past decades, which is attributed to both human activity and internal climate variability[68]. However, the projection of the enhanced precipitation over the TP in our study is derived from the Scenario Model Intercomparison Project participating in the current state-of-the-art CMIP6 models, which mainly reflects the response of the earth system to the anthropogenic forcing such as greenhouse gas concentration[69]. Moreover, although most models and the MME project a wetting TP in the future, there still exists a considerably large inter-model spread in the CMIP6 ensemble (Fig. 3), which has also been discussed in previous studies[70,71]. In addition, accurately simulating TP precipitation is a formidable challenge due to its complex topography[72]. The finding from our study underscores the potential for achieving a more precise projection of TP precipitation, which could contribute to reducing the uncertainty associated with the projected change in SASM circulation.

Methods
CMIP6 data
We use the monthly output from 38 available CMIP6 models (Supplementary Table 1) under the historical experiment and Shared Socioeconomic Pathway (SSP) 5–8.5 scenario[69] in this study. The historical experiment is conducted under the observed historical forcing (e.g., greenhouse gases, solar radiation, aerosols, and land use) and the SSP5-8.5 scenario is forced by the global effective radiation at 8.5 W m^{-2}. To depict the climate change in summer, the variables averaged over JJA during 2050–2099 are compared with those during 1965–2014. The high emission scenario and 50-yr long-term mean adopted here can largely extract the signal of global warming from the future climate, while effectively suppressing the internal variability inherent in the climate system[33,56]. Results from the median emission scenario (SSP2-4.5) are also examined to understand whether our conclusions are sensitive to the choice of scenario, which shows consistent features with SSP5-8.5 (Supplementary Fig. 5). The projected change is considered significant if more than 70% of the individual models agree on the same sign of the MME[73]. All the data are re-gridded into 1° × 1° using bilinear interpolation.

Definition of indices
The South Asian summer monsoon index (SASMI) is defined as the 850-hPa zonal wind averaged over the key region (55°E–100°E, 3°N–15°N) where the low-level westerly wind of SASM significantly weakens[33]. To avoid the sensitivity in selecting monsoon index, two additional monsoon indices are calculated: the vertical wind shear index (VWSI), which is defined as the zonal wind difference between 850 hPa and 200 hPa averaged over 55°E–100°E, 3°N–15°N[1], and the meridional wind shear index (MWSI), which is defined as zonal wind difference between (40°E–80°E,

5°N–15°N) and (70°E–90°E, 20°N–30°N) at 850 hPa[74]. To quantify the intensity of the precipitation, the Tibetan Plateau precipitation index (TPPI), Maritime Continent precipitation index (MCPI), and North Africa precipitation index (NAPI) are defined as the precipitation averaged over (75°E–102°E, 25°N–37°N), (90°E–130°E, 10°S–10°N), and (0°–42°E, 0°N–20°N), respectively.

Inter-model regression

The patterns of climate changes correlated with TP precipitation/latent heating can be obtained by a linear regression analysis among 38 models as follows:

$$Y(m, n) = a(m) \times X(n) + b, \tag{1}$$

where Y is the projected changes, X is the TPPI, a denotes the regression pattern, b is a constant, m is the spatial area (longitude–latitude), and n denotes the number of models. The two-tailed Student's t-test is used to assess the statistical significance.

Apparent heat source

The apparent heat source $(Q1)$[75] is calculated for each model to obtain the three-dimensional structure of the TP heating. The formula of $Q1$ is listed as follows:

$$Q1 = \frac{1}{g}C_p\left(\frac{\partial T}{\partial t} - \omega\sigma + \mathbf{V} \cdot \nabla T\right), \tag{2}$$

where C_p denotes the specific heat capacity at a constant pressure of dry air, T is temperature, ω is vertical velocity, σ represents the static stability, and $\mathbf{V}$ is the horizontal wind.

Moisture budget analysis

Atmospheric moisture budget equation is adopted to reveal the dominant process controlling the future precipitation change[24], which can be written as follows:

$$P' = E' - \left\langle \bar{\omega}\frac{\partial q'}{\partial p}\right\rangle - \left\langle \omega'\frac{\partial \bar{q}}{\partial p}\right\rangle - \left\langle \bar{\mathbf{V}} \cdot \nabla q'\right\rangle - \left\langle \mathbf{V}' \cdot \nabla\bar{q}\right\rangle + \mathrm{NL} + \mathrm{Res}, \tag{3}$$

where P, E, ω, q, $\mathbf{V}$, and p denotes precipitation, evaporation, vertical velocity, specific humidity, horizontal wind, and pressure, respectively. The overbars indicate the historical mean during 1965–2014 and the primes stand for the departure of 2050–2099 mean from the 1965–2014 mean. The symbol $\langle\ \rangle$ denotes the vertical integration from the surface to 100 hPa. Based on the moisture budget equation, the precipitation change (P') can be decomposed into the evaporation change (E'), the thermodynamic change of vertical $(-\langle\bar{\omega}\frac{\partial q'}{\partial p}\rangle)$ and horizontal advection $(-\langle\bar{\mathbf{V}} \cdot \nabla q'\rangle)$, the dynamic change in vertical $(-\langle\omega'\frac{\partial \bar{q}}{\partial p}\rangle)$ and horizontal advection $(-\langle\mathbf{V}' \cdot \nabla\bar{q}\rangle)$, the nonlinear component (NL), and the residual (Res).

Model simulation

The advanced fully-coupled model, the Community Earth System Model version 1.2.2 (CESM 1.2.2) from the National Center for Atmospheric Research (NCAR)[76], is used to explore the effect of TP diabatic heating on the SASM. The resolution of the atmospheric module, the Community Atmosphere Model 4 (CAM4), is 2.5° × 1.9° in longitude and latitude, with 26 vertical levels. For all experiments, solar forcing, ozone concentration, carbon dioxide, and aerosol are maintained at the level of year 2000.

The control run **Con** is integrated for 350 years under the default settings. We further perform a sensitivity experiment **TPheat**, in which other settings are the same as **Con** but the MME-projected change in $Q1$ averaged over the TP (75°E–102°E, 25°N–37°N) in summer is added in the same area uniformly from June to August in every model year. **TPheat** is restarted from the year 251 of **Con** and integrated for 100 years until year 350. Outputs from years 251–350 are analyzed for the two experiments.

References

1. Webster, P. J. & Yang, S. Monsoon and ENSO: selectively interactive systems. *Q. J. R. Meteorol. Soc.* **118**, 877–926 (1992).
2. Webster, P. J. et al. Monsoons: processes, predictability, and the prospects for prediction. *J. Geophys. Res. Oceans* **103**, 14451–14510 (1998).
3. Turner, A. G. & Annamalai, H. Climate change and the south Asian summer monsoon. *Nat. Clim. Change* **2**, 587–595 (2012).
4. Goswami, B. N., Krishnamurthy, V. & Annamalai, H. A broad-scale circulation index for the interannual variability of the Indian summer monsoon. *Q. J. R. Meteorol. Soc.* **125**, 611–633 (1999).
5. Wang, B. & LinHo. Rainy season of the Asian-Pacific summer monsoon. *J. Clim.* **15**, 386–398 (2002).
6. Gao, M. et al. Secular decrease of wind power potential in India associated with warming in the Indian Ocean. *Sci. Adv.* **4**, 1–9 (2018).
7. Krishna, K. et al. Climate impacts on Indian agriculture. *Int. J. Climatol.* **24**, 1375–1393 (2004).
8. Gadgil, S. & Rupa, K. K. The Asian monsoon–agriculture and economy. In: Wang B. (ed) *The Asian monsoon*. Springer, Berlin, pp 651–683 (2006).
9. Hong, J. & Kim, J. Impact of the Asian monsoon climate on ecosystem carbon and water exchanges: a wavelet analysis and its ecosystem modeling implications. *Glob. Chang. Biol.* **17**, 1900–1916 (2011).
10. Mirza, M. M. Q. Climate change, flooding in South Asia and implications. *Reg. Environ. Change* **11**, 95–107 (2011).
11. Zuo, Z. et al. Role of thermal condition over Asia in the weakening Asian summer monsoon under global warming background. *J. Clim.* **25**, 3431–3436 (2012).
12. Huang, X. et al. The recent decline and recovery of Indian summer monsoon rainfall: relative roles of external forcing and internal variability. *J. Clim.* **33**, 5035–5060 (2020).
13. Jin, Q. & Wang, C. A revival of Indian summer monsoon rainfall since 2002. *Nat. Clim. Chang.* **7**, 587–594 (2017).
14. Li, G., Xie, S. P., He, C. & Chen, Z. Western Pacific emergent constraint lowers projected increase in Indian summer monsoon rainfall. *Nat. Clim. Chang.* **7**, 708–712 (2017).
15. Chen, Z. et al. Global land monsoon precipitation changes in CMIP6 projections. *Geophys. Res. Lett.* **47**, e2019GL086902 (2020).
16. Kitoh, A., Yukimoto, S., Noda, A. & Motoi, T. Simulated changes in the Asian summer monsoon at times of increased atmospheric CO$_2$. *J. Meteorol. Soc. Jpn.* **75**, 1019–1031 (1997).
17. Tanaka, H. L., Ishizaki, N. & Nohara, D. Intercomparison of the intensities and trends of Hadley, Walker and monsoon circulations in the global warming projections. *Sci. Online Lett. Atmos.* **1**, 77–80 (2005).
18. Krishnan, R. et al. Will the South Asian monsoon overturning circulation stabilize any further? *Clim. Dyn.* **40**, 187–211 (2013).
19. Wang, B., Yim, S. Y., Lee, J. Y., Liu, J. & Ha, K. J. Future change of Asian-Australian monsoon under RCP 4.5 anthropogenic warming scenario. *Clim. Dyn.* **42**, 83–100 (2014).
20. Sharmila, S., Joseph, S., Sahai, A. K., Abhilash, S. & Chattopadhyay, R. Future projection of Indian summer monsoon variability under climate change scenario: an assessment from CMIP5 climate models. *Glob. Planet Change* **124**, 62–78 (2015).

21. Li, Z., Sun, Y., Li, T., Chen, W. & Ding, Y. Projections of South Asian summer monsoon under global warming from 1.5° to 5 °C. *J. Clim.* **34**, 7913–7926 (2021).

22. Kong, Y., Wu, Y., Hu, X., Li, Y. & Yang, S. Uncertainty in projections of the South Asian summer monsoon under global warming by CMIP6 models: role of tropospheric meridional thermal contrast. *Atmos. Oceanic Sci. Lett.* **15**, 100145 (2022).

23. Held, I. M. & Soden, B. J. Robust responses of the hydrological cycle to global warming. *J. Clim.* **19**, 5686–5699 (2006).

24. Chou, C., Neelin, J. D., Chen, C. A. & Tu, J. Y. Evaluating the 'rich-get-richer' mechanism in tropical precipitation change under global warming. *J. Clim.* **22**, 1982–2005 (2009).

25. Hsu, P. C. et al. Increase of global monsoon area and precipitation under global warming: a robust signal? *Geophys. Res. Lett.* **39**, L06701 (2012).

26. Wang, B., Jin, C. & Liu, J. Understanding future change of global monsoons projected by CMIP6 models. *J. Clim.* **33**, 6471–6489 (2020).

27. Ueda, H., Iwai, A., Kuwako, K. & Hori, M. E. Impact of anthropogenic forcing on the Asian summer monsoon as simulated by eight GCMs. *Geophys. Res. Lett.* **33**, L06703 (2006).

28. Sun, Y., Ding, Y. & Dai, A. Changing links between South Asian summer monsoon circulation and tropospheric land-sea thermal contrasts under a warming scenario. *Geophys. Res. Lett.* **37**, L02704 (2010).

29. Dai, A. et al. The relative roles of upper and lower tropospheric thermal contrasts and tropical influences in driving Asian summer monsoons. *J. Geophys. Res. Atmos.* **118**, 7024–7045 (2013).

30. Wu, Q. et al. Asian summer monsoon responses to the change of land–sea thermodynamic contrast in a warming climate: CMIP6 projections. *Adv. Clim. Chang. Res.* **13**, 205–217 (2022).

31. Ma, J., Xie, S. P. & Kosaka, Y. Mechanisms for tropical tropospheric circulation change in response to global warming. *J. Clim.* **25**, 2979–2994 (2012).

32. Ma, J. & Yu, J. Y. Paradox in South Asian summer monsoon circulation change: lower tropospheric strengthening and upper tropospheric weakening. *Geophys. Res. Lett.* **41**, 2934–2940 (2014).

33. Li, T. et al. Distinctive South and East Asian monsoon circulation responses to global warming. *Sci. Bull.* **67**, 762–770 (2022).

34. May, W. Potential future changes in the Indian summer monsoon due to greenhouse warming: analysis of mechanisms in a global time-slice experiment. *Clim. Dyn.* **22**, 389–414 (2004).

35. Stowasser, M., Annamalai, H. & Hafner, J. Response of the South Asian summer monsoon to global warming: mean and synoptic systems. *J. Clim.* **22**, 1014–1036 (2009).

36. Yanai, M. et al. Seasonal heating of the Tibetan Plateau and its effects on the evolution of the Asian summer monsoon. *J. Meteorol. Soc. Jpn.* **70**, 319–351 (1992).

37. Wu, G. et al. The influence of mechanical and thermal forcing by the Tibetan Plateau on Asian climate. *J. Hydrometeorol.* **8**, 770–789 (2007).

38. Boos, W. & Kuang, Z. Dominant control of the South Asian monsoon by orographic insulation versus plateau heating. *Nature* **463**, 218–223 (2010).

39. Molnar, P., Boos, W. & Battisti, D. Orographic controls on climate and paleoclimate of Asia: thermal and mechanical roles for the Tibetan Plateau. *Ann. Rev. Earth Planet. Sci.* **38**, 77–102 (2010).

40. He, B., Wu, G., Liu, Y. & Bao, Q. Astronomical and hydrological perspective of mountain impacts on the Asian summer monsoon. *Sci. Rep.* **5**, 17586 (2015).

41. Duan, A., Hu, D., Hu, W. & Zhang, P. Precursor effect of the Tibetan Plateau heating anomaly on the seasonal march of the East Asian summer monsoon precipitation. *J. Geophys. Res. Atmos.* **125**, 1–20 (2020).

42. Liu, Y. et al. Land–atmosphere–ocean coupling associated with the Tibetan Plateau and its climate impacts. *Natl Sci. Rev.* **7**, 534–552 (2020).

43. Wang, J. et al. Optimal meridional positions of the Tibetan Plateau for intensifying the Asian summer monsoon. *J. Clim.* **35**, 3861–3875 (2022).

44. Xie, Y. et al. Oceanic repeaters boost the global climatic impact of the Tibetan Plateau. *Sci. Bull.* **68**, 2225–2235 (2023).

45. Yu, W. et al. Potential impact of winter–spring North Atlantic tripole SSTAs on the following autumn–winter El Niño–Southern Oscillation: bridging role of the Tibetan Plateau. *Geophys. Res. Lett.* **50**, 1–13 (2023).

46. Yeh, T. C., Luo, S. W. & Chu, P. C. The wind structure and heat balance in the lower troposphere over Tibetan Plateau and its surrounding. *Acta Meteor. Sin.* **28**, 108–121 (1957).

47. Flohn, H. Large-scale aspects of the "summer monsoon" in South and East Asia. *J. Meteor. Soc. Jpn.* **75**, 180–186 (1957).

48. Duan, A. M. & Wu, G. X. Role of the Tibetan Plateau thermal forcing in the summer climate patterns over subtropical Asia. *Clim. Dyn.* **24**, 793–807 (2005).

49. Wang, Z. et al. Tibetan Plateau heating as a driver of monsoon rainfall variability in Pakistan. *Clim. Dyn.* **52**, 6121–6130 (2019).

50. Abe, M., Kitoh, A. & Yasunari, T. An evolution of the Asian summer monsoon associated with mountain uplift–simulation with the MRI atmosphere-ocean coupled GCM. *J. Meteor. Soc. Jpn.* **81**, 909–933 (2003).

51. Wu, G. et al. Thermal controls on the Asian summer monsoon. *Sci. Rep.* **2**, 1–7 (2012).

52. Lu, M., Yang, S., Wang, J., Wu, Y. & Jia, X. Response of regional Asian summer monsoons to the effect of reduced surface albedo in different Tibetan Plateau domains in idealized model experiments. *J. Clim.* **34**, 7023–7036 (2021).

53. IPCC. Climate Change 2023: Synthesis Report. Contribution of Working Groups I, II and III to the Sixth Assessment Report of the Intergovernmental Panel on Climate Change [Core Writing Team, H. Lee and J. Romero (eds.)]. IPCC, Geneva, Switzerland, pp 35–115 (2023).

54. Zhou, T., Gao, J., Zhao, Y., Zhang, L. & Zhang, W. Water vapor transport processes on Asian Water Tower (in Chinese). *Bull. Chin. Acad. Sci.* **34**, 1210–1219 (2019).

55. You, Q. et al. Warming amplification over the Arctic Pole and Third Pole: trends, mechanisms and consequences. *Earth. Sci. Rev.* **217**, 103625 (2021).

56. He, C., Wang, Z., Zhou, T. & Li, T. Enhanced latent heating over the Tibetan Plateau as a key to the enhanced East Asian summer monsoon circulation under a warming climate. *J. Clim.* **32**, 3373–3388 (2019).

57. Chen, Z. et al. Observationally constrained projection of Afro-Asian monsoon precipitation. *Nat. Commun.* **13**, 1–12 (2022).

58. Hu, J. & Duan, A. Relative contributions of the Tibetan Plateau thermal forcing and the Indian Ocean Sea surface temperature basin mode to the interannual variability of the East Asian summer monsoon. *Clim. Dyn.* **45**, 2697–2711 (2015).

59. Jiang, X., Li, Y., Yang, S., Yang, K. & Chen, J. Interannual variation of summer atmospheric heat source over the Tibetan Plateau and the role of convection around the Western Maritime Continent. *J. Clim.* **29**, 121–138 (2016).

60. Luo, X. et al. Characteristics of atmospheric heat sources in the Tibetan plateau-tropical Indian ocean region. *J. Trop. Meteor.* **27**, 70–80 (2021).

61. Wang, Z., Yang, S., Luo, H. & Li, J. Drying tendency over the southern slope of the Tibetan Plateau in recent decades: role of a CGT-like atmospheric change. *Clim. Dyn.* **59**, 2801–2813 (2022).

62. He, B., Liu, Y., Wu, G., Wang, Z. & Bao, Q. The role of air–sea interactions in regulating the thermal effect of the Tibetan–Iranian Plateau on the Asian summer monsoon. *Clim. Dyn.* **52**, 4227–4245 (2019).

63. Wang, Z., Duan, A. & Yang, S. Potential regulation on the climatic effect of Tibetan Plateau heating by tropical air–sea coupling in regional models. *Clim. Dyn.* **52**, 1685–1694 (2019).
64. Wu, G., Zhuo, H., Wang, Z. & Liu, Y. Two types of summertime heating over the Asian large-scale orography and excitation of potential-vorticity forcing I. Over Tibetan Plateau. *Sci. China Earth Sci.* **59**, 1996–2008 (2016).
65. Endo, H., Kitoh, A. & Ueda, H. A unique feature of the Asian summer monsoon response to global warming: the role of different land-sea thermal contrast change between the lower and upper troposphere. *Sci. Online Lett. Atmosphere* **14**, 57–63 (2018).
66. Yue, S. et al. Mechanisms of the decadal variability of monsoon rainfall in the southern Tibetan Plateau. *Environ. Res. Lett.* **16**, 014011 (2020).
67. Zhao, D., Zhang, L. & Zhou, T. Detectable anthropogenic forcing on the long-term changes of summer precipitation over the Tibetan Plateau. *Clim. Dyn.* **59**, 1939–1952 (2022).
68. Jiang, J. et al. Precipitation regime changes in High Mountain Asia driven by cleaner air. *Nature* **623**, 544–549 (2023).
69. O'Neill, B. C. et al. The Scenario Model Intercomparison Project (ScenarioMIP) for CMIP6. *Geosci. Model. Dev.* **9**, 3461–3482 (2016).
70. Zhao, Y., Zhou, T., Zhang, W. & Li, J. Change in precipitation over the Tibetan Plateau projected by weighted CMIP6 models. *Adv. Atmos. Sci.* **39**, 1133–1150 (2022).
71. Qiu, H., Zhou, T., Chen, X., Wu, B. & Jiang, J. Understanding the diversity of CMIP6 models in the projection of precipitation over Tibetan Plateau. *Geophys. Res. Lett.* **51**, e2023GL106553 (2024).
72. Xie, Z. & Wang, B. Summer heat sources changes over the Tibetan Plateau in CMIP6 models. *Environ. Res. Lett.* **16**, 064060 (2021).
73. Power, S. B., Delage, F., Colman, R. & Moise, A. Consensus on twenty-first-century rainfall projections in climate models more widespread than previously thought. *J. Clim.* **25**, 3792–3809 (2012).
74. Wang, B., Wu, R. & Lau, K.-M. Interannual variability of the Asian summer monsoon: contrasts between the Indian and the western North Pacific-East Asian monsoons. *J. Clim.* **14**, 4073–4090 (2001).
75. Yanai, M., Esbensen, S. & Chu, J. Determination of bulk properties of tropical cloud clusters from large-scale heat and moisture budgets. *J. Atmos. Sci.* **30**, 611–627 (1973).
76. Hurrell, J. et al. The community earth system model: a framework for collaborative research. *Bull. Am. Meteorol. Soc.* **94**, 1339–1360 (2013).

Acknowledgements

Author contributions

Z.W. conceived the idea for the study, Z.W. and S.Y. supervised the work, H.L. analyzed the data, plotted the figures, and drafted the paper. All authors discussed the results throughout the whole process and contributed to the revision.

Competing interests

The authors declare no competing interests.

Additional information

Supplementary information The online version contains supplementary material available at https://doi.org/10.1038/s41612-024-00653-x.

Correspondence and requests for materials should be addressed to Ziqian Wang or Song Yang.

Reprints and permissions information is available at http://www.nature.com/reprints

Publisher's note Springer Nature remains neutral with regard to jurisdictional claims in published maps and institutional affiliations.